Chemical Engineering Science 247 (2022) 117041

Contents lists available at ScienceDirect

Chemical Engineering Science

journal homepage: www.elsevier.com/locate/ces

Determination of nitration kinetics of *p*-Nitrotoluene with a homogeneously continuous microflow

Jing Song [1], Yongjin Cui [1], Lin Sheng, Yujun Wang, Chencan Du, Jian Deng *, Guangsheng Luo *

State Key Laboratory of Chemical Engineering, Department of Chemical Engineering, Tsinghua University, Beijing 100084, China

HIGHLIGHTS

- The characteristics of nitration hinder the accurate determination of kinetics.
- Constructing a continuous-flow microreactor system to obtain kinetics of nitration.
- Determining p-nitrotoluene nitration kinetics by homogeneous reaction in the system.
- Establishing a general method to obtain the values of $C_{NO_2^+}/C_{HNO_3}$.

ARTICLE INFO

Article history:
Received 19 May 2021
Received in revised form 9 July 2021
Accepted 21 August 2021
Available online 25 August 2021

Keywords:
P-nitrotoluene nitration
Homogeneous
Kinetics
Continuous
Microflow

ABSTRACT

The kinetics of *p*-nitrotoluene nitration with mixed acid is important to industrial process design and safety control. However, it's difficult to acquire accurate kinetic data and no kinetics study has ever been reported before because of fast, highly exothermic and heterogeneous characteristics. In this work, a continuous-flow microreactor system including a micromixer, a capillary reactor and an online quenching module was designed to carry out the nitration under a homogeneous reaction condition. The homogeneous nitration can completely eliminate mass transfer resistance between phases, and accurately control reaction temperature and residence time in the continuous-flow microreactor system. The observed reaction rate constants separately based on HNO_3 and NO_2^+, pre-exponential factor and activation energy of *p*-nitrotoluene nitration were obtained and a general method was established to collect kinetics data for such a kind of fast and highly exothermal nitration reactions.

1. Introduction

2,4-dinitrotoluene (24-DNT) is an important intermediate for the production of dyes and explosives, which can be produced through *p*-nitrotoluene (4-MNT) nitration with mixed acid (Scheme 1). (Kulkarni, 2014; Olah et al., 1989; Rahaman et al., 2007; Sullivan et al., 2020) The kinetics study is very important to industrial process design and prevent the thermal runaway because nitration is fast and highly exothermic. But it is difficult to obtain the accurate kinetic data because of the following reasons: (1) compared to the reaction time, the time of quenching reaction and sampling cannot be ignored in the traditional stirred tank reactor. It could result in inaccurate determination of residence time; (2) the constant temperature process is very difficult to be maintained because of the characteristic of highly exothermic reaction; (3) the reaction is coupled strongly with mass transfer in the liquid–liquid heterogeneous system. (Hompson and Eegers, 1990; Zaldivar et al., 1995; Zeegers, 1993) It is believed that the nitration process occurs almost exclusively in the aqueous phase. (Cox and Strachan, 1972a, b; Thompson and Zeegers, 1989) HNO_3 reacts with concentrated H_2SO_4 to generate NO_2^+ firstly. 4-MNT diffuses through the organic phase to the aqueous phase to react with NO_2^+ to form 24-DNT. There is always mass transfer resistance in the diffusion process. (Quadros et al., 2004) The use of concentrated H_2SO_4 could further increase the mass transfer resistance because of its high viscosity. Therefore, in order to obtain accurate kinetics data of nitration, a method of quenching reaction at milliseconds, and a reactor with excellent mass and heat transfer performances are required.

Kinetic studies of nitration have attracted the interest of many researchers. (Barbosa et al., 2006; Su et al., 2011; Sullivan et al., 2020) Kinetic studies of many aromatic compounds have been reported in the literatures such as toluene, (Chapman et al.,

* Corresponding authors.
E-mail addresses: jiandeng@tsinghua.edu.cn (J. Deng), gsluo@tsinghua.edu.cn (G. Luo).
[1] Jing Song and Yongjin Cui contributed equally to this work.

https://doi.org/10.1016/j.ces.2021.117041
0009-2509/

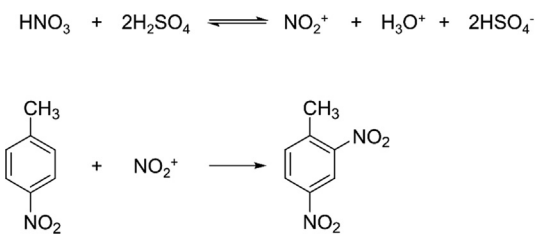

Scheme 1. Nitration of 4-MNT with mixed acid to form 24-DNT.

1974; Cox and Strachan, 1972b; Su et al., 2011) benzene, (Biggs and White, 2010; Quadros et al., 2005) nitrotoluene, (Modak and Juvekar, 1995; Nunziata et al., 1983; Su et al., 2011; Westheimer and Kharasch, 1946) and chlorobenzene. (Cox and Strachan, 1971) However, an accurate kinetics study of 4-MNT nitration has not ever been reported before. More studies on the kinetics of this reaction should be performed.

Microreactor could have excellent transfer and mixing performances because of its micron or submicron characteristic dimensions. (Chen et al., 2021; Cui et al., 2020; Han et al., 2019; Sheng et al., 2021; Yan et al., 2021) In addition, the residence time can be accurately controlled in a continuous-flow microreactor system. (Barbosa et al., 2005) These advantages in kinetics studies have been proven by many reported heterogeneous nitration reactions. (Kulkarni et al., 2009; Lan and Lu, 2021; Li et al., 2017; Wen et al., 2018) However, the mass transfer resistance in liquid–liquid reaction system cannot be eliminated completely. It is reported that 4-MNT has a certain solubility in 95% H_2SO_4 at 303 K without sulfonation, and a homogeneous nitration reaction system can be formed. (Andreozzi et al., 1993; Rahaman et al., 2010; Rahaman et al., 2007) In a homogeneous reaction system, the mass transfer resistance between phases could be eliminated. The high mass ratio of sulfuric acid to 4-MNT can not only ensure the formation of homogenous solution, but also effectively reduce the adiabatic temperature rise of the system, which is an effective method to control the reaction temperature. Therefore, more accurate kinetic data of homogeneous 4-MNT nitration in a continuous-flow microreactor system may be obtained. Unfortunately, this work has not ever been tested before.

In this study, a continuous-flow microreactor system including a micromixer, a capillary reactor and an online quenching module has been constructed to determine the kinetics of 4-MNT nitration under a homogeneous condition. The requirement of constant temperature was satisfied by adjusting the mass ratio of H_2SO_4 to 4-MNT. It can be proved by the calculation of the adiabatic temperature rise of the system. The mass transfer resistance between phases can be eliminated completely. In the microreactor system, the effect of mixing performance, temperature, residence time and molar ratio of reactants on nitration were investigated in detail and the reaction kinetic parameters including observed reaction rate constants separately based on HNO_3 and NO_2^+, preexponential factor and activation energy as well as their confidence intervals were obtained.

2. Experimental

2.1. Chemicals and materials

4-MNT (99%) and 24-DNT (99%), and nitrobenzene (99.8%) were purchased from Aladdin and Macklin, respectively. MeOH (99.5%), H_2SO_4 (98%), HNO_3 (98%) were supplied by Shanghai Titan Scientific Co., Ltd., Beijing Tong Guang Fine Chemicals Company and Sinopharm Chemical Reagent Beijing Co., Ltd., respectively. H_2SO_4 (less than98%) was prepared by diluting H_2SO_4 (98%) with deionized water.

2.2. Experimental procedures and equipment

The homogeneous solution of 4-MNT dissolved in specific concentration H_2SO_4 (0.5 g / (0.5 + 160) g) was prepared by stirring for 12 h. According to the molar ratio of nitric acid and 4-MNT, nitric acid was also dissolved in 160 g the same concentration H_2SO_4 to obtain the mixed acid.

The continuous-flow microreactor system (Fig. 1) contains two high-pressure syringe pumps (Chemyx fusion 6000, America), pretreatment coiled capillaries (stainless steel, inner diameter of 0.5 mm, length of 1 m), micromixers (stainless three-way, inner diameter of 0.15 mm, 0.25 mm and 0.5 mm), a capillary microreactor (PTFE, inner diameter of 0.5 mm, 0.75 mm, and 1.0 mm), and one metering pump (2 PB-3020, Beijing Xingda, China). The pretreatment, reaction and quenching modules were immersed in a temperature-controlled bath (CORIO CD-200F, Julabo, Germany).

The homogeneous solution and mixed acid were delivered through high-pressure syringe pumps at the same volume flow rate, respectively. The two fluids flow separately through the pretreatment coiled capillaries to reach a preset temperature and through micromixer 1 to microreactor system for several seconds. The change in reaction residence time was realized by adjusting the length of the capillary microchannel. The reaction was quenched by water at milliseconds at the outlet of the microchannel reactor.

2.3. Analysis

Since H_2SO_4 in the quenched sample has been sufficiently diluted, it could not react with methanol. Therefore, all the organic products and acids were dissolved in methanol and analyzed by ultra-performance liquid chromatography (Waters, ACQUITY UPLC I-CLASS System, column: PFP Column, 1.8 μm, 3 mm × 50 mm, America, mobile phase: V_{H2O}/V_{MeOH} = 0.65/0.35, flow rate: 0.2 mL/min, injection volume: 1 μL). The column temperature was 30 °C and the detection wavelength of the UV detector was 200–300 nm. The composition of product was quantitatively analyzed by the internal standard method and nitrobenzene was also dissolved in methanol as an internal standard.

$$f_i = \frac{A_s/m_s}{A_{ri}/m_{ri}} \tag{1}$$

where i and s represent components and internal standard substance, respectively. A and m are the integral area and the mass of nitrobenzene, respectively. f_i is the relative correction factor for component i. Before each measurement of the composition of samples, the relative correction factors of 4-MNT and 24-DNT were determined first. All these experiments were repeated at least three times to determine the reproducibility.

The conversion of 4-MNT is calculated by equation (2):

$$X_{4\text{-MNT}} = 1 - \frac{\omega_{4\text{-MNT}}}{\omega_{4\text{-MNT}} + \omega_{2,4\text{-,DNT}} \times \frac{M_{4\text{-MNT}}}{M_{2,4-DNT}}} \tag{2}$$

where X, ω and M are the conversion, mass fraction and molecular weight, respectively.

The reaction residence time is calculated by equation (3):

$$t = \frac{V}{Q_h + Q_m} \tag{3}$$

where t is the reaction residence time, and V is the volume of the microchannel. Q_h and Q_m are the volume flow rates of the homogeneous solution and mixed acid solution, respectively.

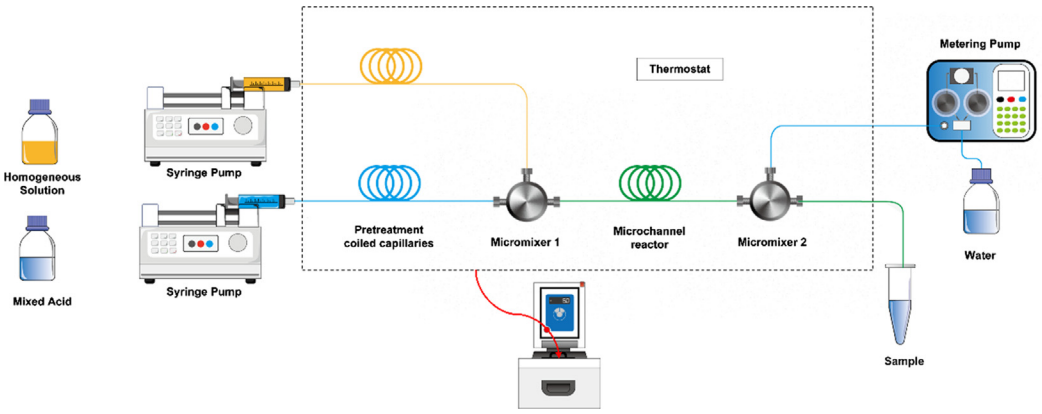

Fig. 1. Schematic overview of the experimental equipment.

The adiabatic temperature rise is calculated by equation (4):

$$\Delta T = \frac{Q_r \times n_{4\text{-MNT}} X_{4\text{-MNT}}}{c_{p\text{-}H_2SO_4} \times m_{H_2SO_4}} = \frac{Q_r}{M_{4\text{-MNT}} \times c_{p\text{-}H_2SO_4}} \cdot \frac{X_{4\text{-MNT}}}{k_m} \quad (4)$$

Where ΔT is the adiabatic temperature rise, Q_r is the reaction heat of 4-MNT nitration reaction, $n_{4\text{-MNT}}$ is the initial molar of 4-MNT, $c_{p\text{-}H_2SO_4}$ is the specific heat capacity of H_2SO_4, $m_{H_2SO_4}$ is the total mass of H_2SO_4 in the microchannel, and $k_m = m_{H_2SO_4}/m_{4-MNT}$.

2.4. Determination of the solubility of 4-MNT in H_2SO_4

The solubility was determined using the following procedure. The mixture of 4-MNT and 88% H_2SO_4 ($m_{4-MNT}/m_{H_2SO_4} = 1/2$) was stirred for 12 h at 288 K and rested for 24 h. Next, the mixture was separated into an organic phase and aqueous phase through separating funnel. The analysis samples were prepared by dissolving the aqueous phase in methanol. The content of 4-MNT in the aqueous phase was analyzed by the above-mentioned UPLC method and convert to the value of solubility.

3. Results and discussion

3.1. Solubility of 4-MNT in H_2SO_4

It is a prerequisite that 4-MNT can be dissolved in H_2SO_4 to form a homogeneous nitration reaction system. The solubility of 4-MNT in 88% H_2SO_4 at 288 K was shown to equal 0.1503 g per 1 g H_2SO_4. Therefore, in the range of solubility, 4-MNT can be completely dissolved in 88% H_2SO_4 at the given temperature to form a homogeneous solution. According to the previous literature, (Rahaman et al., 2010) the solubility of aromatic compounds in H_2SO_4 increases with increasing of H_2SO_4 concentration and temperature. In addition, the sulfonation side reaction did not occur even in 95% H_2SO_4 at 308 K, as shown in the **Supplementary Material** (Figure S2). Therefore, the solubility research proved that the homogeneous nitration of 4-MNT in mixed acid is feasible under expected experimental conditions.

3.2. Mixing performance of the continuous-flow microreactor system

In the homogeneous nitration of 4-MNT in the microreaction process, the sufficient mixing is still vital to such a fast reaction although the influence of the mass transfer resistance between phases on nitration was eliminated completely. The reaction rate will be hindered by the poor mixing in kinetics studies. Therefore, sufficient mixing is necessary for determination of accurate kinetics data. To achieve the best mixing effect in the selected microreactor system, the effects of the inner diameter of the micromixer and microreactor, and the fluid flow rate on the conversion of 4-MNT were investigated, respectively.

First, the micromixers 1 (with inner diameters of 0.15 mm, 0.25 mm and 0.5 mm) and the capillary microreactors (with inner diameters of 0.5 mm, 0.75 mm and 1.0 mm) were used to explore the optimal equipment that could achieve a better mixing effect. The results are shown in Fig. 2(a) and 2(b). The results prove that as the inner diameters of the micromixer and microreactor increase, the conversion of 4-MNT decreases under the same reaction conditions. Under the same flow rate, the smaller the inner diameter is, the greater the fluid velocity is. The turbulence in the fluid will be more intense. The more sufficient the fluid is mixed, the more conducive to the occurrence of the reaction. Therefore, a better mixing effect was achieved in the micromixer and microreactor with smaller inner diameters. According to the above results, a micromixer with an inner diameter of 0.15 mm and a microreactor with an inner diameter of 0.5 mm were utilized for the next step of the research.

To achieve the best mixing effect in the selected micromixer and microreactor, the influence of the fluid flow rate on the conversion of 4-MNT was explored. The results are shown in Fig. 2(c). According to the results, when the fluid volume flow rate is lower than 1.0 mL/min, the conversion of 4-MNT increases with increasing of the fluid volume flow rate. When the fluid volume flow rate is higher than 1.0 mL/min, with the increase in the volume flow rate, the conversion of 4-MNT is almost unchanged. The results show that when the volume flow rate is increased to a certain value in the selected reaction devices, the mixing effect achieved in the selected micromixer and microreactor has almost no further influence on the reaction rate. Therefore, all the subsequent kinetics experiments were studied under the optimal mixing conditions.

3.3. Effect of molar ratio

The effect of the molar ratio of HNO_3 to 4-MNT was investigated at 293 K and the residence time of 7.07 s. The results are shown in Fig. 3, indicating that with increasing of molar ratio, the conversion of 4-MNT increases. According to the reported literature, (Edwards and Fawcett, 1994; Edwards et al., 1995) when the most of the mixed acid is occupied by H_2SO_4, as the concentration of HNO_3 increases, the concentration of NO_2^+ increases. Furthermore, the low proportion of water in the mixed acid is conducive to the protonation of HNO_3. When the proportion of HNO_3 in the mixed acid is large, the concentration of NO_2^+ will decrease with increasing of HNO_3. In this work, a large amount of H_2SO_4 and a small amount of HNO_3 were used to prepare the mixed acid. The oxidation

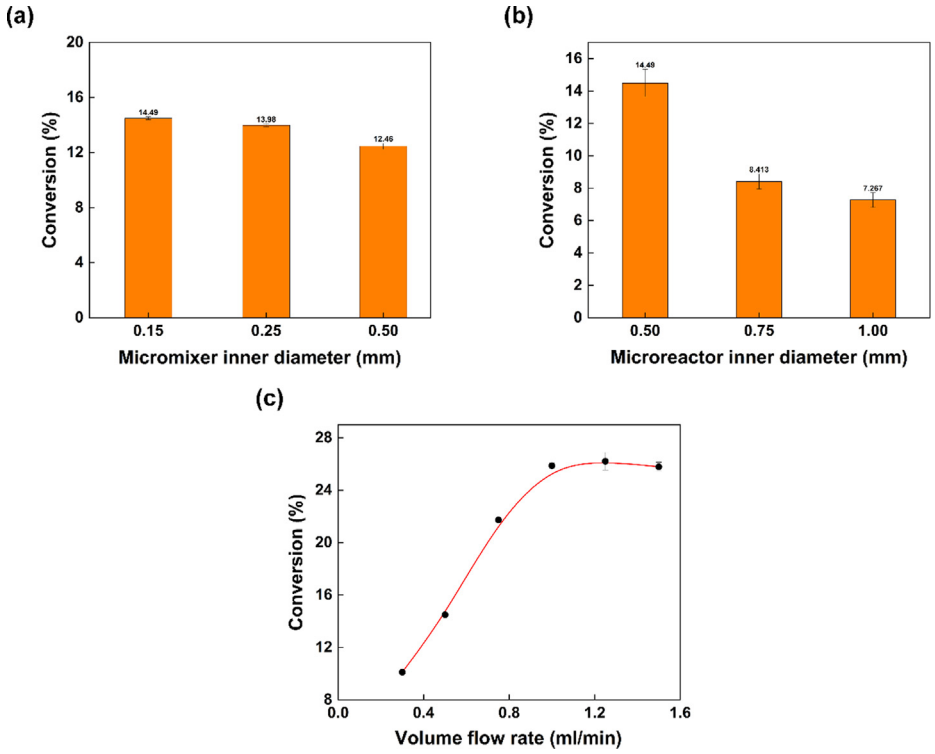

Fig. 2. Effect of (a) micromixer inner diameter, (b) microreactor inner diameter, (c) fluid flow rate on 4-MNT conversion.

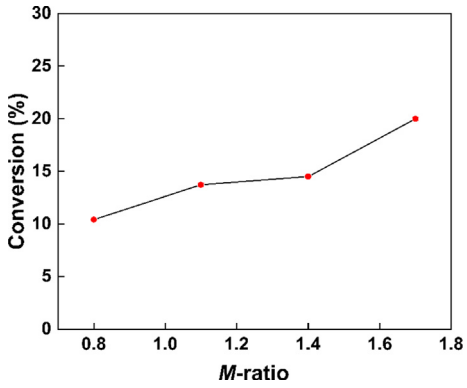

Fig. 3. Conversion variation of 4-MNT with molar ratio of HNO_3 to 4-MNT.

reaction of HNO_3 can be reduced in this system. (Deno et al., 1961; Ross et al., 1983) Therefore, as the molar ratio increases, the reaction rate appears faster. The effect of the molar ratio on the observed reaction rate constant can also be reflected in the reaction rate equation. Furthermore, due to the constant consumption of NO_2^+ in the reaction process, a higher molar ratio is conducive to supplementation with NO_2^+. Therefore, a high molar ratio and high concentration of H_2SO_4 are more favorable to nitration.

3.4. Determination of the observed reaction rate constant based on HNO_3

It has been proven that a homogeneous nitration reaction is a second-order reaction. The reaction rate of 4-MNT nitration can be described as equation (5):

$$r = k_{obs} C_{4\text{-MNT}} C_{HNO_3} \tag{5}$$

where k_{obs} is the observed reaction rate constant based on HNO_3 and $C_{4\text{-MNT}}$ and C_{HNO3} are the concentrations of 4-MNT and HNO_3, respectively. Equation (5) can be transformed in terms of the conversion of 4-MNT and described by the following rate equations:

$$r = k_{obs} C^0_{4\text{-MNT}} (1 - X_{4\text{-MNT}}) \left(C^0_{HNO_3} - C^0_{4\text{-MNT}} X_{4\text{-MNT}} \right) \tag{6}$$

$$r = k_{obs} C^0_{4\text{-MNT}} (1 - X_{4\text{-MNT}}) (M - X_{4\text{-MNT}}) \tag{7}$$

$$r = -\frac{dC_{4-MNT}}{dt} = C^0_{4-MNT} \frac{dX_{4-MNT}}{dt} \tag{8}$$

where $X_{4\text{-MNT}}$ is the conversion of 4-MNT, $C^0_{HNO_3}$ and $C^0_{4\text{-MNT}}$ are the initial concentrations of HNO_3 and 4-MNT in the homogeneous solution, respectively, and $M = C^0_{HNO_3}/C^0_{4\text{-MNT}}$, t is the reaction residence time. By integrating Equations (7)-(8), we can obtain

$$\ln\left[\frac{M - X_{4\text{-MNT}}}{M(1 - X_{4\text{-MNT}})}\right] = k_{obs}\left(C^0_{HNO_3} - C^0_{4\text{-MNT}}\right) t \tag{9}$$

Therefore, a plot of $\ln\left[\frac{M - X_{4\text{-MNT}}}{M(1 - X_{4\text{-MNT}})}\right]$ versus t is a straight line, and the slope equals $k_{obs}\left(C^0_{HNO_3} - C^0_{4\text{-MNT}}\right)$. Next, the observed rate constant based on HNO_3, k_{obs}, can be calculated from the slope.

At different temperatures and H_2SO_4 concentrations, Fig. 4 describes the variation in the conversion of 4-MNT with reaction residence time. To ensure that constant temperature conditions were satisfied in this work, the adiabatic temperature rise of each process was calculated. According to the results, the adiabatic temperature rises of all processes were less than 1 K. Therefore, it can be believed that requirement of the accurate temperature control was satisfied. The detailed results are given in the **Supplementary Material** (Table S2). Fig. 5 shows the relationship between $\ln\left[\frac{M - X_{4\text{-MNT}}}{M(1 - X_{4\text{-MNT}})}\right]$ and residence time (t). The values of k_{obs} and its

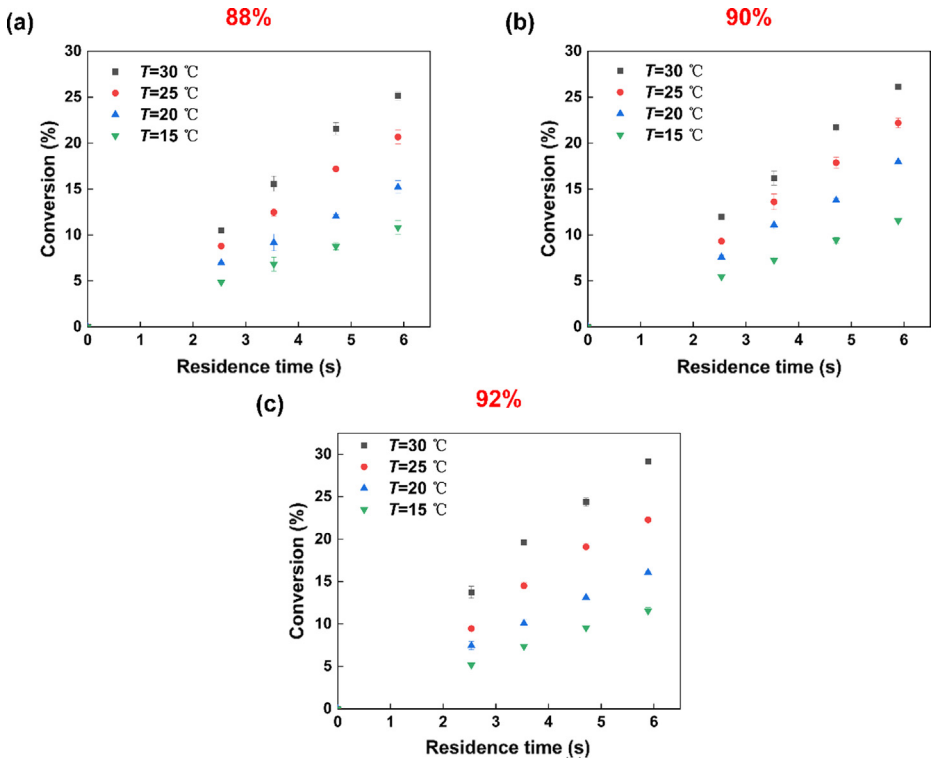

Fig. 4. Effect of the residence time, temperature and concentration of H_2SO_4 on conversion. (a) 88% H_2SO_4, (b)90% H_2SO_4, (c) 92% H_2SO_4.

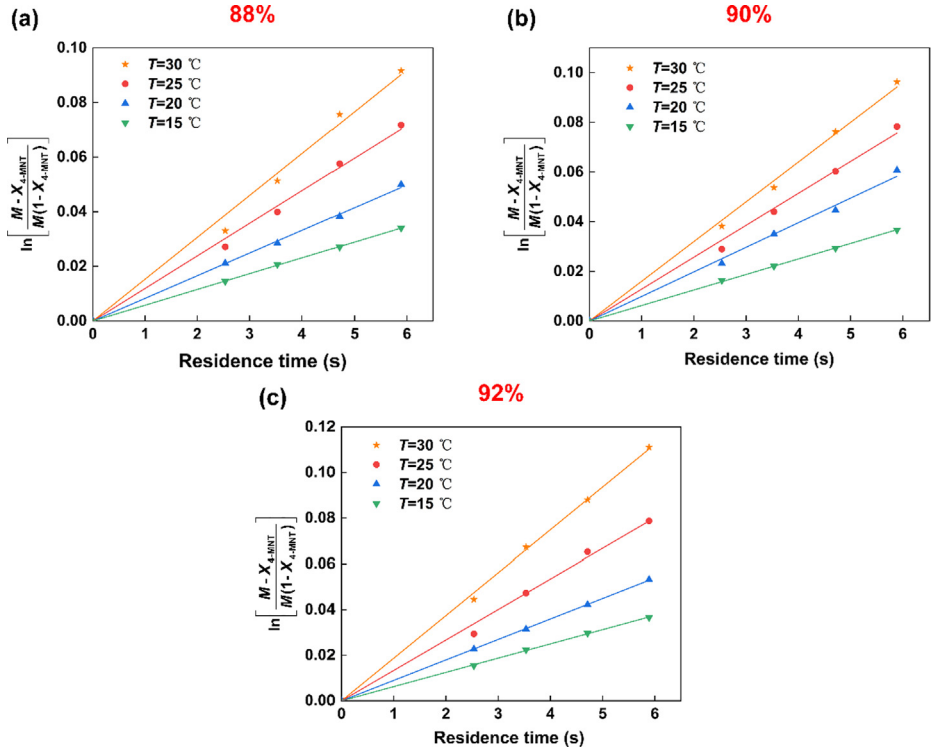

Fig. 5. Determination of the observed reaction rate constant k_{obs} at different temperatures and H_2SO_4 concentrations. (a) 88% H_2SO_4. (b) 90% H_2SO_4. (c) 92% H_2SO_4.

95% confidence intervals are shown in the Table 1. At all H_2SO_4 concentrations, with increasing of reaction temperature, the conversion of 4-MNT is greater under the same reaction residence time. This result shows that as the temperature increases, the reaction rate increases. The results of Fig. 5 show that the excellent linear relationships are obtained. This finding demonstrates that the results are in accordance with the second order reaction trend. It has been proven that the observed reaction rate constant based on HNO_3 is a strong function of H_2SO_4 concentration. (Nunziata et al., 1983; Westheimer and Kharasch, 1946) It can be seen that

Table 1
Values and 95% confidence intervals of k_{obs} at different temperatures and H_2SO_4 concentrations.

Mass fraction of H_2SO_4 (%)	Temperature (°C)	$k_{obs}\times10^2$ (L mol^{-1} s^{-1})
88	15	35.20 ± 0.36
	20	50.95 ± 1.58
	25	74.99 ± 4.20
	30	97.04 ± 7.31
90	15	37.50 ± 0.48
	20	61.31 ± 3.51
	25	80.37 ± 4.53
	30	99.06 ± 4.17
92	15	37.68 ± 0.54
	20	54.11 ± 0.42
	25	82.38 ± 4.81
	30	113.94 ± 3.13

The 95% confidence interval of k_{obs} is from the linear fit.

k_{obs} increases with increasing of H_2SO_4 concentration. Decreases in the proportion of water in mixed acid is more conducive to the production of NO_2^+.

3.5. Determination of the observed reaction rate constant based on NO_2^+

It is well known that the attack of NO_2^+ on the aromatic compounds is the rate-determining step in the nitration reaction. In addition, NO_2^+ is the real nitrating agent instead of HNO_3. Therefore, to determine the law of 4-MNT nitration and explain the dependence of the observed reaction rate constant on the H_2SO_4 concentration, the determination of the observed reaction rate constant based on NO_2^+ is necessary. In Equation (5), the reaction rate is expressed by the concentration of HNO_3. When the reaction rate is expressed by the concentration of NO_2^+, the reaction rate equation can be transformed as Equation (10).

$$r = k_2^* C_{4\text{-MNT}} C_{NO_2^+} \tag{10}$$

where k_2^* is the observed second-order reaction rate constant related to the concentration of NO_2^+ and $C_{NO_2^+}$ is the concentrations of NO_2^+.

According to the Brønsted-Bjerrum rate law (transition-state theory), (Olah et al., 1989) the reaction rate equation can be written as follows:

$$r = k^* C_{4\text{-MNT}} C_{NO_2^+} \frac{\gamma_{4\text{-MNT}}\gamma_{NO_2^+}}{\gamma^*} \tag{11}$$

where k^* is the observed reaction rate constant based on NO_2^+ and it is a thermodynamic parameter that is a function of temperature. $\gamma_{4\text{-MNT}}$, $\gamma_{NO_2^+}$ and γ^* are the activity coefficients of 4-MNT, NO_2^+ and the transition intermediate, respectively. According to the literature reported by Marziano *et al.*, (Marziano et al., 1984) Equation (11) can be transformed by the M_c function which is expressed by the H_2SO_4 concentration as follows:

$$r = k^* C_{4\text{-MNT}} C_{NO_2^+} 10^{nMc} \tag{12}$$

where n is a thermodynamic parameter that depends on the aromatic compound. The values of n will be different for different aromatic compounds. The M_c function, which represents the acidity of H_2SO_4 is used to depict the change in the activity coefficients.

By comparing Equations (5) and (12), the relationship between k_{obs} and k^* can be described as follows:

$$k^* = \frac{k_{obs}}{10^{nM_c}} \frac{C_{HNO_3}}{C_{NO_2^+}} \tag{13}$$

Next, by rearranging Equation (13), we can obtain

$$\lg k_{obs} - \lg\left(C_{NO_2^+}/C_{HNO_3}\right) = \lg k^* + nM_c \tag{14}$$

According to Equation (14), to obtain the values of k^* and n, the values of $C_{NO_2^+}/C_{HNO_3}$ and M_c function should be determined first. Marziano *et al.* proved that at a specific temperature, the M_c function exclusively depends on the H_2SO_4 concentration. The values of the M_c function at 298 K can be calculated by polynomial fitting to the data in the literature reported by Marziano *et al.* (Marziano et al., 1973) In the H_2SO_4 concentration range between 15.2 and 18.4 mol/L, the polynomial is given as follows:

$$-M_c = 2.16\times10^{-4}C_{H_2SO_4}^5 - 1.27\times10^{-2}C_{H_2SO_4}^4 + 0.28C_{H_2SO_4}^3 - 2.73C_{H_2SO_4}^2 + 10.6C_{H_2SO_4} \tag{15}$$

The result of polynomial fitting is given in the **Supplementary Material** (Figure S1). Therefore, the values of the M_c function with different H_2SO_4 concentrations can be determined at 298 K by Equation (15). (Marziano et al., 1981) The values at other temperatures can be calculated by equation (16):

$$M_c(T) = M_c(298\text{K})\left[\frac{200}{T} + 0.3292\right] \tag{16}$$

The values of $C_{NO_2^+}/C_{HNO_3}$ are crucial for determining the values of k^*. It has been proven that $C_{NO_2^+}/C_{HNO_3}$ is a function of temperature and H_2SO_4 concentration. Many researchers have determined

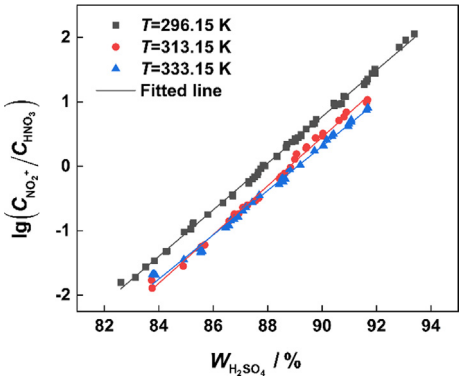

Fig. 6. Variation of $\lg\left(C_{NO_2^+}/C_{HNO_3}\right)$ with the H_2SO_4 concentration at different temperatures and fitted lines.

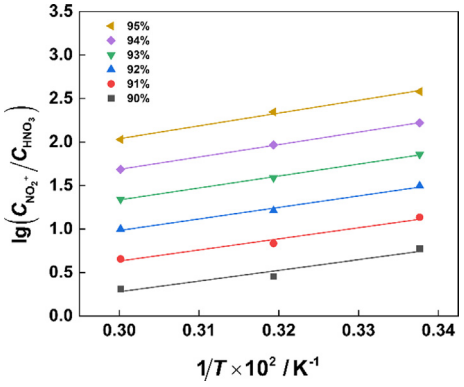

Fig. 7. Variation of $\lg\left(C_{NO_2^+}/C_{HNO_3}\right)$ with temperature at different H_2SO_4 concentrations and fitted lines.

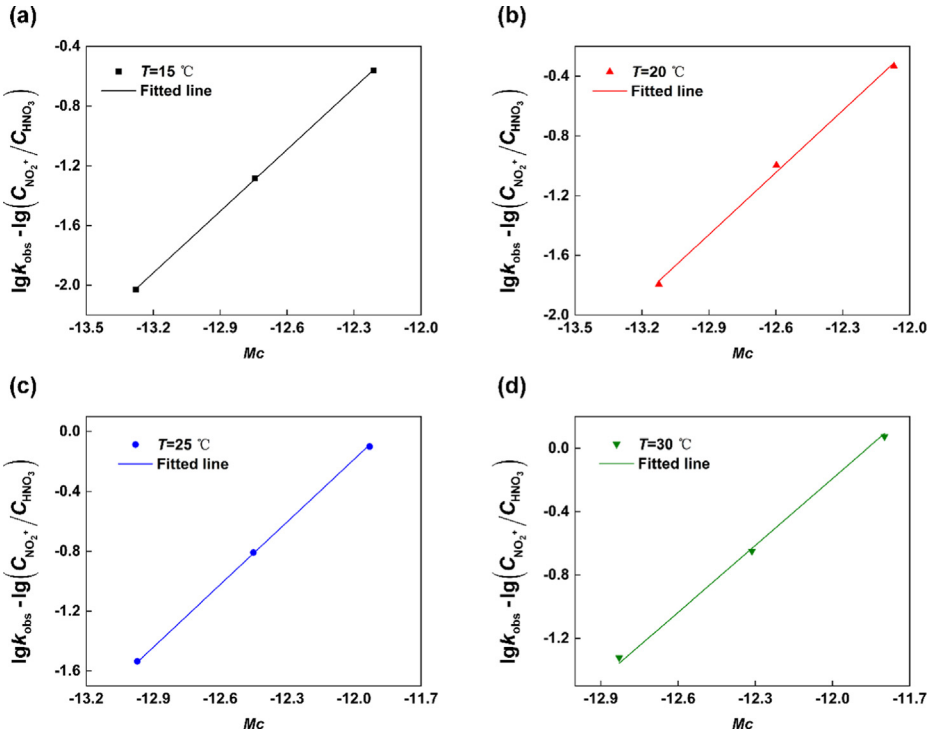

Fig. 8. Determination of the thermodynamic parameter n and k^* at different temperatures. (a) T = 15 °C, (b) T = 20 °C, (c) T = 25 °C, (d) T = 30 °C.

the value of $C_{NO_2^+}/C_{HNO_3}$ at different temperatures and H_2SO_4 concentrations. To obtain reliable values of $C_{NO_2^+}/C_{HNO_3}$, a mathematical model is proposed in this work.

First, according to the values of $C_{NO_2^+}/C_{HNO_3}$ reported in the previous literature, (Marziano et al., 1998; Sapoli et al., 1985) by plotting the values of $\lg\left(C_{NO_2^+}/C_{HNO_3}\right)$ versus mass fraction of H_2SO_4 at the given temperatures in the literature, the results are shown in Fig. 6. It can be observed that the experimental data are fitted well with the straight line at the three temperatures. Next, the values of $\lg\left(C_{NO_2^+}/C_{HNO_3}\right)$ under the H_2SO_4 concentration used in the experiment can be calculated according to the fitted model. The results of the values of $\lg\left(C_{NO_2^+}/C_{HNO_3}\right)$ under experimental conditions are given in the **Supplementary Material** (Table S1). Therefore, at all H_2SO_4 concentrations, the values of $\lg\left(C_{NO_2^+}/C_{HNO_3}\right)$ corresponding to the three temperatures were obtained. Next, by plotting the values of $\lg\left(C_{NO_2^+}/C_{HNO_3}\right)$ versus $1/T$ at different H_2SO_4 concentrations, the results are shown in Fig. 7.

After determining the values of the M_c function and $\lg\left(C_{NO_2^+}/C_{HNO_3}\right)$, according to Equation (14), by plotting the $\lg k_{obs} - \lg\left(C_{NO_2^+}/C_{HNO_3}\right)$ versus M_c function at different temperatures, the results are shown in Fig. 8. All data are fitted well by straight lines. Therefore, the thermodynamic parameter n and k^* can be calculated by the slopes and intercepts of these straight lines, respectively. The values of n and $\lg k^*$ obtained at different temperatures are presented in Table 2.

By combining Equations (5), (10) and (12), the relationship between k_2^* and k_{obs}, k_2^* and k^* can be written as follows:

$$k^*_{2,exp} = k_{obs}\frac{C_{HNO_3}}{C_{NO_2^+}} \tag{17}$$

$$k^*_{2,cal} = k^* 10^{nM_c} \tag{18}$$

According to Equation (17), $k^*_{2,exp}$ can be expressed by k_{obs} and $C_{NO_2^+}/C_{HNO_3}$. The values of k_{obs} and $C_{NO_2^+}/C_{HNO_3}$ have been directly determined through experiments. According to Equation (18), $k^*_{2,cal}$ can be expressed by k^* and n. The values of k^* and n have been

Table 2
Values and 95% confidence intervals of n and $\lg k^*$ at different temperatures.

Temperature (°C)	n	$\lg k^*$
15	1.377 ± 0.001	16.258 ± 0.018
20	1.385 ± 0.007	16.412 ± 0.090
25	1.396 ± 0.002	16.566 ± 0.028
30	1.408 ± 0.006	16.707 ± 0.078

The 95% confidence intervals of n and $\lg k^*$ *are* from the linear fit.

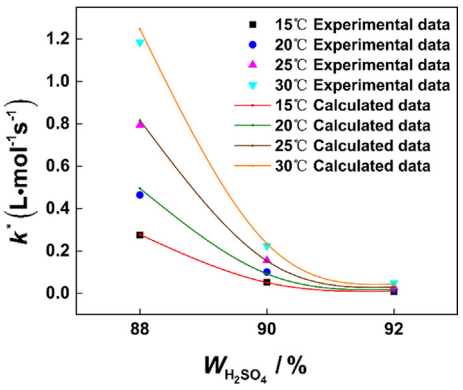

Fig. 9. Comparison of experimental and calculated values of k_2^* at different H_2SO_4 strengths and temperatures.

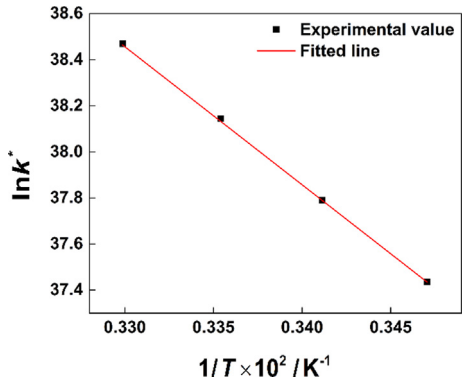

Fig. 10. Arrhenius plot of lnk^* versus 1/T.

Table 3
Values and 95% confidence intervals of the preexponential factor and activation energy.

Factors	Values
E_a	50.207 ± 1.496 kJ mol^{-1}
ln$A$	58.393 ± 0.609

The 95% confidence intervals of E_a *and* ln$A$ are from the linear fit.

determined from the linear fit. The comparison between $k^*_{2,exp}$ and $k^*_{2,cal}$ at different H_2SO_4 strengths and temperatures is shown in Fig. 9. The calculated values are in excellent agreement with the experimental values and prove the validation of the model.

The research scope of molar ratio of HNO_3 to 4-MNT was expanded for further analyzing the correlation of conversion and molar ratio and verifying the applicability of the kinetic model. When the molar ratio was 2, the conversion of 4-MNT was 22.81 % under the same temperature and residence time, and higher than that at a molar ratio of 1.7. The result is consistent with the conclusion that a high molar ratio is more favorable to nitration. According to the kinetic model, the calculated conversion was 23.51%. It demonstrates that the kinetic model is applicable when the molar ratio is changed.

After obtaining the values of k^* at different temperatures, the activation energy for the attack of NO_2^+ on 4-MNT molecules and the preexponential factor can be obtained. The relationship between k^* and the activation energy can be described by the Arrhenius equation as follows:

$$k^* = A\exp\left(-\frac{E_a}{RT}\right) \tag{19}$$

where A is the preexponential factor and E_a is the activation energy. R is the molar gas constant. By plotting lnk^* versus 1/T, a straight line can be obtained. Next, the value of E_a can be calculated by the slope of the fitted line, and the value of A can be calculated by the intercept of the fitted line. The results are shown in Fig. 10. The values and 95% confidence intervals are shown in Table 3.

4. Conclusions

In this work, a complete continuous-flow microreactor system has been constructed. The kinetics of 4-MNT nitration were studied by means of a homogeneous reaction in the continuous-flow microreactor. The solubility of 4-MNT in concentrated H_2SO_4 solution was measured first to ensure that the reaction was carried out under homogeneous conditions. The constant temperature condition can be proven by the adiabatic temperature rise of each process below 1 K. The observed reaction rate constants based on HNO_3 were obtained. This finding proves that the reaction rate is highly dependent on the H_2SO_4 strength and temperature. Next, a complete kinetic model was established to describe this reaction. The observed reaction rate constant based on NO_2^+ is a parameter that is not affected by the change in H_2SO_4 concentration. And the results at different temperatures were calculated by the values of $\lg\left(C_{NO_2^+}/C_{HNO_3}\right)$ and M_c function. A general method to obtain the values of $C_{NO_2^+}/C_{HNO_3}$ was proposed in this work. The preexponential factor and activation energy as well as their confidence intervals were obtained. The activation energy of 4-MNT nitration is 50.207 ± 1.496 kJ/mol. This model first reported the preexponential factor and activation energy of the reaction of 4-MNT nitration. By comparing the calculated values and experimental values, model validation was proven. The kinetics study method can be applied to processes with similar reaction mechanisms. This model can help to deeply understand the whole process of 4-MNT nitration and will be used to optimize the operating conditions. Furthermore, it is expected to achieve more efficient and faster determination of reaction kinetics of similar nitration process by combining the method of kinetics study and the automation technology in our future work.

Funding information

National Natural Science Foundation of China, Grant/Award Number: 21,991,104.

CRediT authorship contribution statement

Jing Song: Writing – original draft, Investigation, Methodology. **Yongjin Cui:** Validation, Formal analysis. **Lin Sheng:** Software. **Yujun Wang:** Writing – review & editing. **Chencan Du:** Writing – review & editing. **Jian Deng:** Writing – review & editing, Conceptualization. **Guangsheng Luo:** Writing – review & editing, Conceptualization, Supervision.

Declaration of Competing Interest

The authors declare that they have no known competing financial interests or personal relationships that could have appeared to influence the work reported in this paper.

Acknowledgements

This work was financially supported by the National Natural Science Foundation of China (Grant No.21991104).

Appendix A. Supplementary material

Supplementary data to this article can be found online at https://doi.org/10.1016/j.ces.2021.117041.

Reference

Andreozzi, R., Insola, A., Aquila, T., Caprio, V., 1993. Kinetics of benzonitrile nitration with mixed acid under homogeneous conditions. Int. J. Chem. Kinet. 25 (9), 771–776. https://doi.org/10.1002/kin.550250907.

Barbosa, I.V.M., Merquior, D.M., Peixoto, F.C., 2006. Estimation of kinetic and mass-transfer parameters for cellulose nitration. AIChE J. 52 (10), 3549–3554. https://doi.org/10.1002/(ISSN)1547-590510.1002/aic.v52:1010.1002/aic.10974.

Barbosa, I.V.M., Merquior, D.M., Peixoto, F.C., 2005. Continuous modelling and kinetic parameter estimation for cellulose nitration. Chem. Eng. Sci. 60 (19), 5406–5413. https://doi.org/10.1016/j.ces.2005.05.029.

Biggs, R.D., White, R.R., 2010. Rate of nitration of benzene with mixed acid. AIChE J. 2 (1), 26–33. https://doi.org/10.1002/aic.690020106.
Marziano, N.C., Tomasin, A., Tortato, C., Zaldivar, J.M., 1998. Thermodynamic nitration rates of aromatic compounds. Part 4. Temperature dependence in sulfuric acid of HNO3→NO2+ equilibrium, nitration rates and acidic properties of the solvent †. J. Chem. Soc. Perkin Trans. (9), 1973–1982 https://doi.org/10.1039/a802521e.
Chapman, J.W., Cox, P.R., Strachan, A.N., 1974. Two phase nitration of toluene—III. Chem. Eng. Sci. 29 (5), 1247–1251. https://doi.org/10.1016/0009-2509(74)80124-7.
Chen, Y., Sheng, L., Deng, J., Luo, G., 2021. Geometric effect on gas-liquid bubbly flow in capillary-embedded T-junction microchannels. Ind. Eng. Chem. Res. 60 (12), 4735–4744. https://doi.org/10.1021/acs.iecr.1c00262.
Cox, P.R., Strachan, A.N., 1971. Two phase nitration of chlorobenzene. Chem. Eng. Sci. 26 (7), 1013–1018. https://doi.org/10.1016/0009-2509(71)80014-3.
Cox, P.R., Strachan, A.N., 1972a. Two-phase nitration of toluene. Part II. Chem. Eng. J. 4 (3), 253–261. https://doi.org/10.1016/0300-9467(72)80022-4.
Cox, P.R., Strachan, A.N., 1972b. Two phase nitration of toluene — I. Chem. Eng. Sci. 27 (3), 457–463. https://doi.org/10.1016/0009-2509(72)87001-5.
Cui, Y., Li, Y., Wang, K., Deng, J., Luo, G., 2020. Determination of Dynamic Interfacial Tension during the Generation of Tiny Droplets in the Liquid-Liquid Jetting Flow Regime. Langmuir 36 (45), 13633–13641. https://doi.org/10.1021/acs.langmuir.0c02459.
Deno, N.C., Peterson, H.J., Sacher, E., 1961. NITRIC ACID EQUILIBRIA IN WATER—SULFURIC ACID1. J. Phys. Chem. 65 (2), 199–201. https://doi.org/10.1021/j100820a002.
Edwards, H.G.M., Fawcett, V., 1994. Quantitative Raman spectroscopic studies of nitronium ion concentrations in mixtures of sulphuric and nitric acids. J. Mol. Struct. 326, 131–143. https://doi.org/10.1016/0022-2860(94)85013-5.
Edwards, H.G.M., Turner, J.M.C., Fawcett, V., 1995. Raman spectroscopic study of nitronium ion formation in mixtures of nitric acid, sulfuric acid and water. J. Chem. Soc Faraday Trans. 91, 1439–1443. https://doi.org/10.1039/FT9959101439.
Han, C.L., Hu, Y.P., Wang, K., Luo, G.S., 2019. Preparation and in-situ surface modification of CaCO3 nanoparticles with calcium stearate in a microreaction system. Powder Technol. 356, 414–422. https://doi.org/10.1016/j.powtec.2019.08.054.
hompson, M.J., Eegers, P.J., 1990. Studies on the two-phase nitration of phenols (part 2). Tetrahedron 46 (7), 2661–2674. https://doi.org/10.1016/S0040-4020(01)82044-5.
Kulkarni, A.A., 2014. Continuous flow nitration in miniaturized devices. Beilstein J. Org. Chem. 10, 405–424. https://doi.org/10.3762/bjoc.10.38.
Kulkarni, A.A., Kalyani, V.S., Joshi, R.A., Joshi, R.R., 2009. Continuous Flow Nitration of Benzaldehyde. Org Process Res Dev. 13 (5), 999–1002. https://doi.org/10.1021/op900129w.
Lan, Z., Lu, Y., 2021. Continuous nitration of o-dichlorobenzene in micropacked-bed reactor: process design and modelling. J. Flow Chem. 11 (2), 171–179. https://doi.org/10.1007/s41981-020-00132-3.
Li, L., Yao, C., Jiao, F., Han, M., Chen, G., 2017. Experimental and kinetic study of the nitration of 2-ethylhexanol in capillary microreactors. Chem. Eng. Process. 117, 179–185. https://doi.org/10.1016/j.cep.2017.04.005.
Marziano, N.C., Cimino, G.M., Passerini, R.C., 1973. The M activity coefficient function for acid–base equilibria. Part I. New methods for estimating pka values for weak bases. J. Chem. Soc Perkin Trans. 2, 1915–1922. https://doi.org/10.1039/P29730001915.
Marziano, N.C., Sampoli, M., Pinna, F., Passerini, A., 1984. Thermodynamic nitration rates of aromatic compounds. Part 2. Linear description of rate profiles for the nitration of aromatic compounds in the range 40–98 wt% sulphuric acid. J. Chem. Soc. Perkin Trans. 2, 1163–1166. https://doi.org/10.1039/P29840001163.
Marziano, N.C., Tomasin, A., Traverso, P.G., 1981. The Mc activity coefficient function for acid–base equilibria. Part 5. The Mc activity coefficient for a reliable estimate of thermodynamic values. J. Chem. Soc. Perkin Trans. 2, 1070–1075. https://doi.org/10.1039/P29810001070.
Modak, S.Y., Juvekar, V.A., 1995. Role of Interfacial Reaction in Heterogeneous Aromatic Nitration. Ind. Eng. Chem. Res. 34 (12), 4297–4309. https://doi.org/10.1021/ie00039a021.
Nunziata, C., Marziano, Marco, Sampoli, 1983. A simple linear description of rate profiles for the nitration of aromatic compounds in the critical range 80–98 wt% sulphuric acid. J. Chem. Soc., 523–524. https://doi.org/10.1039/C39830000523.
Olah, G.A., Malhotra, R., Narang, S.C., 1989. NITRATION: Methods and Mechanisms. Across Conventional Lines. https://doi.org/10.1142/9789812791405_0192.
Quadros, P.A., Oliveira, N.M.C., Baptista, C.M.S.G., 2004. Benzene nitration: validation of heterogeneous reaction models. Chem. Eng. Sci. 59 (22-23), 5449–5454. https://doi.org/10.1016/j.ces.2004.07.107.
Quadros, P.A., Oliveira, N.M.C., Baptista, C.M.S.G., 2005. Continuous adiabatic industrial benzene nitration with mixed acid at a pilot plant scale. Chem. Eng. J. 108 (1-2), 1–11. https://doi.org/10.1016/j.cej.2004.12.022.
Rahaman, M., Mandal, B., Ghosh, P., 2010. Nitration of nitrobenzene at high-concentrations of sulfuric acid: Mass transfer and kinetic aspects. AIChE J. 56, 737–748. https://doi.org/10.1002/aic.11989.
Rahaman, M., Mandal, B.P., Ghosh, P., 2007. Nitration of nitrobenzene at high-concentrations of sulfuric acid. AIChE J. 53, 2476–2480. https://doi.org/10.1002/aic.11222.
Ross, D.S., Kuhlmann, K.F., Malhotra, R., 1983. Studies in aromatic nitration. 2. Nitrogen14 NMR study of the nitric acid/nitronium ion equilibrium in aqueous sulfuric acid. J. Am. Chem. Soc. 105 (13), 4299–4302. https://doi.org/10.1021/ja00351a030.
Sapoli, M., De Santis, A., Marziano, N.C., Pinna, F., Zingales, A., 1985. Equilibria of nitric acid in sulfuric and perchloric acid at 25.degree.C by Raman and UV spectroscopy. J. Phys. Chem. 89, 2864–2869. https://doi.org/10.1021/j100259a032.
Sheng, L., Chen, Y., Wang, K., Deng, J., Luo, G., 2021. General rules of bubble formation in viscous liquids in a modified step T-junction microdevice. Chem. Eng. Sci. 239, 116621. https://doi.org/10.1016/j.ces.2021.116621.
Su, Y., Zhao, Y., Jiao, F., Chen, G., Yuan, Q., 2011. The intensification of rapid reactions for multiphase systems in a microchannel reactor by packing microparticles. AIChE J. 57 (6), 1409–1418. https://doi.org/10.1002/aic.12367.
Sullivan, F., Simon, L., Ioannidis, N., Patel, S., Ophir, Z., Gogos, C., Jaffe, M., Tirmizi, S., Bonnett, P., Abbate, P., 2020. Chemical reaction modeling of industrial scale nitrocellulose production for military applications. AIChE J. 66 (7). https://doi.org/10.1002/aic.v66.710.1002/aic.16234.
Thompson, M.J., Zeegers, P.J., 1989. A theoretical study on the two-phase nitration of phenols. Tetrahedron 45 (1), 191–202. https://doi.org/10.1016/0040-4020(89)80046-8.
Wen, Z., Yang, M., Zhao, S., Zhou, F., Chen, G., 2018. Kinetics study of heterogeneous continuous-flow nitration of trifluoromethoxybenzene. React. Chem. Eng. 3 (3), 379–387. https://doi.org/10.1039/C7RE00182G.
Westheimer, F.H., Kharasch, M.S., 1946. The Kinetics of Nitration of Aromatic Nitro Compounds in Sulfuric Acid1. J. Am. Chem. Soc. 68, 1871–1876. https://doi.org/10.1021/ja01214a001.
Yan, Z., Tian, J., Wang, K., Nigam, K.D.P., Luo, G., 2021. Microreaction processes for synthesis and utilization of epoxides: A review. Chem. Eng. Sci. 229, 116071. https://doi.org/10.1016/j.ces.2020.116071.
Zaldivar, J.M., Molga, E., Alós, M.A., Hernández, H., Westerterp, K.R., 1995. Aromatic nitrations by mixed acid. Slow liquid-liquid reaction regime. Chem. Eng. Process. 34 (6), 543–559. https://doi.org/10.1016/0255-2701(95)04111-7.
Zeegers, P.J., 1993. Nitration of phenols: A two-phase system. J. Chem. Educ. 70 (12), 1036. https://doi.org/10.1021/ed070p1036.